

# Switching off chaos in two-dimensional optical cavities

C. Xu,<sup>1, 2, a)</sup> L. -G. Wang,<sup>1, b)</sup> and P. Sebbah<sup>2, c)</sup>

<sup>1)</sup>*Zhejiang Province Key Laboratory of Quantum Technology and Device, Department of Physics, Zhejiang University, Hangzhou 310027, China*

<sup>2)</sup>*Department of Physics, The Jack and Pearl Resnick Institute for Advanced Technology, Bar-Ilan University, Ramat-Gan 5290002, Israel*

(Dated: 5 June 2025)

Chaos is generally considered a nuisance, inasmuch as it prevents long-term predictions in physical systems. Here, we present an easily accessible approach to undo deterministic chaos in arbitrary two-dimensional optical chaotic billiards, by introducing spatially varying refractive index therein. The landscape of refractive index is obtained by a conformal transformation from an integrable billiard. Our study shows that this approach is robust to small fluctuations. We show further that trajectory rectification can be realized by relating chaotic billiards with non-Euclidean billiards. Finally, we illustrate the universality of this approach by extending our investigations to arbitrarily deformed optical billiards. This work not only contributes in controlling chaos, but provides a novel pathway to the design of billiards and microcavities with desired properties and functionalities.

Chaos is omnipresent in contemporary science. In a chaotic system, a small uncertainty in an initial state can rapidly lead to significant fluctuations in the long-term behavior of a physical system, which makes deterministic predictability (nearly) impossible. Back to 1990s, attempts to overcome this nuisance had already been proposed, ranging from the design of synchronized chaotic systems for private communication<sup>1</sup> to the stabilization of periodic orbits by precisely applying periodic kicks<sup>2,3</sup>. In the past decades, chaos has been used to improve the abilities of optical resonators and microcavities<sup>4–12</sup>, such as enhancing energy storage<sup>7</sup>, chaos-assisted broadband momentum transformation<sup>11</sup>, and suppressing lasing instabilities<sup>12</sup>. Despite the ingeniousness of these specific systems, manipulating chaos reveals itself delicate and hardly generalizable. In this Letter, we take a radically opposed approach and propose to recover predictability by switching off chaos in an otherwise chaotic billiard.

Billiard systems have long been recognized as a fundamental platform in the study of classical and quantum chaos, because they can realize a broad range of degrees of chaos. A two-dimensional (2D) flat (table) billiard is a closed and hard-wall region within which particles or light rays move freely except for specular collisions on its boundary. For flat billiards, the essential mechanism of chaos merely lies in the dispersing (defocusing) nature of convex (concave) boundaries<sup>13</sup>. Recently, a different pathway has been proposed for chaos engineering: curvature, by constructing billiards on a deformed torus<sup>14</sup>. Shortly afterwards, we proved a complete equivalence between non-Euclidean billiards which are built on arbitrary surfaces of revolution and flat billiards with nonuniform distribution of refractive index<sup>15</sup>, a parallel mathematically rooted in a conformal coordinate transformation<sup>16</sup>. Building on this equivalence, we demonstrated that the degree of chaos can actually be controlled by simply tuning a geometrical parameter of the curved surface,

or equivalently, the distribution of refractive index in the 2D billiard. In a very recent research, Fan et al. experimentally demonstrated a dynamical transition between regular and chaotic modes in a quarter Bunimovich stadium by optically manipulating a Kerr gate<sup>17</sup>. With the ultrafast interaction of a femtosecond laser with photonic cavity, Bruck et al. realized ultrafast order-to-chaos transitions in silicon photonic crystal chips<sup>18</sup>. These studies stimulate us to come up with an interesting question: can we have a universal method to turn off chaos in a chaotic optical cavity/billiard with fixed boundaries? Such a method to manipulate the chaotic nature of a system would be extremely useful in practical applications such as laser directivity and emission control.

In this Letter, we propose an original and practical approach to transform chaotic flat billiards into integrable ones. By introducing a non-uniform refractive index landscape in the flat chaotic resonator, we bend light rays propagation in the billiards such that the dispersing (defocusing) effect of the boundaries is elaborately offset. We show that the distribution of refractive index can be obtained by an optical transformation from an integrable circular billiard. We tested the robustness of this distribution against chaos, and found the system surprisingly poorly sensitive to index fluctuation. Interestingly, when considering transformation from non-Euclidean billiards rather than 2D integrable billiards, we show that it is expected to force all the trajectories in the new 2D cavity to be not only regular, but also periodic, in light of geometrical properties of geodesics on the curved surfaces. Finally, the universality of this chaos switch-off approach is discussed by taking into consideration chaotic billiards of arbitrary deformed boundaries.

We consider a typical family of chaotic billiards, the Robnik billiards, as an example, and portray its degree of chaos through Poincaré surface of section (SOS). It is well known that Poincaré SOS can record the states of a light ray [to be exact, the position  $\zeta$  and the tangent angular momentum  $\sin \chi$ , where  $\chi$  is the angle between the incident direction and the normal of the boundary, sketched in the upper right panels of Figs. 1(c) and (e)] everytime it collides on the boundary, and essentially represents the history of the dynamical system. By this means, it presents the structure of the phase space, and

<sup>a)</sup>Electronic mail: chennixu@zju.edu.cn

<sup>b)</sup>Electronic mail: lgwang@zju.edu.cn

<sup>c)</sup>Electronic mail: patrick.sebbah@biu.ac.il

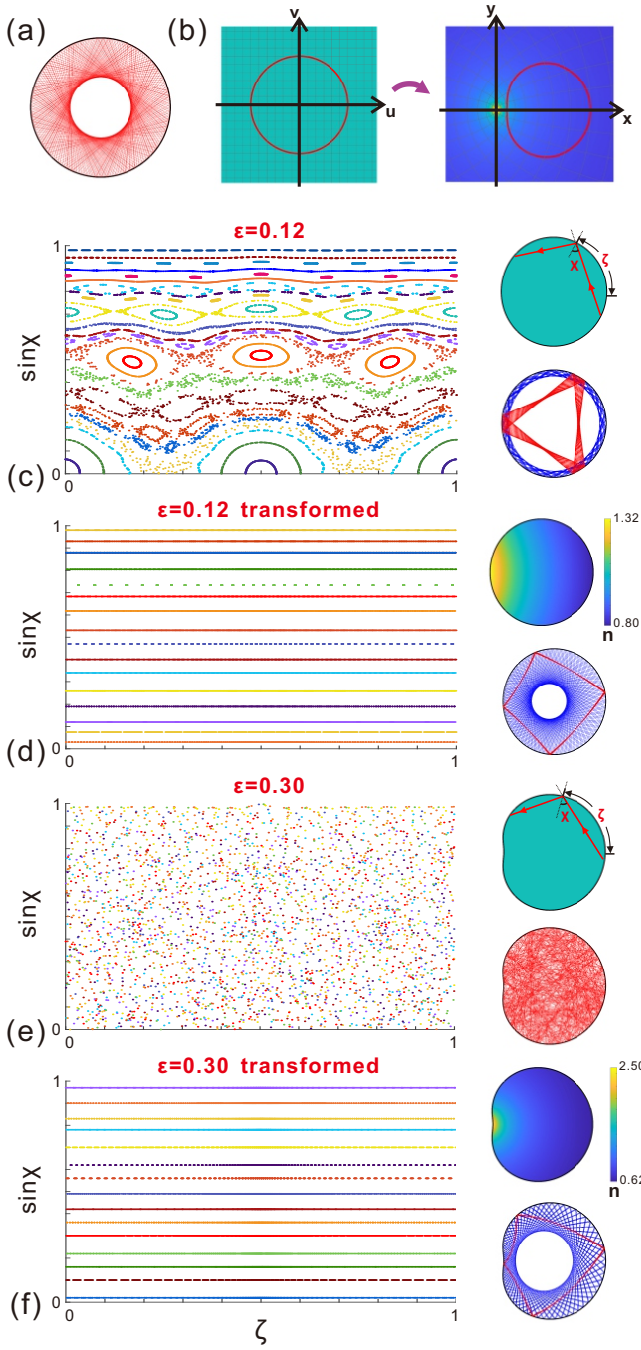


FIG. 1. (a) A circular billiard. The thin red line denotes a typical trajectory. (b) The original space  $uv$  (left) and the conformally transformed space  $xy$  with distribution of refractive index (right). (c-f) (Left) Poincaré SOSs of (c,e) the uniform and (d,f) the corresponding transformed Robnik billiards with (c,d)  $\epsilon = 0.12$  and (e,f)  $\epsilon = 0.3$ . (Upper right) Distribution of refractive index in the billiard, and (lower right) typical trajectories in the Robnik billiards which present themselves in Poincaré SOS with corresponding color. In (c), the blue trajectory is a whispering gallery orbit, and the red trajectory is a quasi-periodic orbit. In (e), the red trajectory is chaotic and explores ergodically the whole billiard. In (d,f), the nonuniform distributions of refractive index restore the regularity of trajectories in the transformed billiards.

therefore is a robust mathematical tool to probe and investigate chaos in billiards. The boundaries of Robnik billiards is analytically defined as<sup>19</sup>

$$x = \cos \Theta + \epsilon \cos (2\Theta), y = \sin \Theta + \epsilon \sin (2\Theta), \quad (1)$$

with  $\Theta$  running from 0 to  $2\pi$ , and constant  $\epsilon$  determining the degree of deformation relative to the circular shape. When  $\epsilon = 0$ , Eq. (1) describes a circular billiard shown in Fig. 1(a). Owing to the conservation of angular momentum, any free particle or light ray is forbidden to enter a central circular area whose radius equals to the absolute value of its initial angular momentum<sup>20</sup>, and hence their trajectories naturally form a caustic. Another consequence of the angular momentum conservation is the invariance of tangential momentum (i.e.,  $\sin \chi$ ). A planar circular billiard is integrable, since the number of constants of motion equals to the dimension of the system. Therefore all the trajectories in the four-dimensional (4D) phase space are restricted in a 2D manifold, whose shape, according to a theorem of topology, is a 2D torus<sup>21</sup>. When visualized in the Poincaré SOS, each trajectory is a horizontal line with constant  $\sin \chi$ . When  $\epsilon$  increases and the billiard is progressively deformed [see Fig. 1(c)], the previous horizontal lines become wavy to different extent, especially at small  $|\sin \chi|$ . Some of them turn into a curved narrow band with disordered grainy texture, while for others, numerous series of "islands" take shape which correspond to stable periodic orbits. When  $\epsilon$  gets even larger, as in Fig. 1(e), the island chains break up gradually, and trajectories explore the whole phase space stochastically and ergodically. It is clear that when  $\epsilon = 0.30$ , such billiard is already fully chaotic.

In order to undo chaos and transform such partially or fully chaotic billiards into integrable, we propose to relate them to an integrable circular billiard through a conformal coordinate transformation. Mathematically, when both the 2D original space and transformed space are denoted by complex numbers (say,  $w = u + iv$  and  $z = x + iy$ , respectively), and the transformation is in the form of a complex analytical function  $z = f(w)$ , then the Cauchy-Riemann condition is satisfied and such transformation is automatically conformal<sup>16</sup>. Based on this concept, the boundary of the Robnik billiard can be obtained from the boundary of a circular billiard by applying a quadratic transformation<sup>19,22</sup>

$$z = w + \epsilon w^2 + \gamma, \quad (2)$$

where  $\gamma$  is a complex constant. The distribution of refractive index in the transformed space is given by

$$n(x, y) = n_0 \left| \frac{dw}{dz} \right| \quad (3a)$$

$$= \frac{n_0}{\sqrt{4\epsilon}} \left\{ \left[ x + \frac{1}{4\epsilon} - \text{real}(\gamma) \right]^2 + [y - \text{imag}(\gamma)]^2 \right\}^{-\frac{1}{4}} \quad (3b)$$

with  $n_0$  the refractive index of the circular billiard. For practical realization of the index landscape, the distribution of refractive index can be proportionally modified by changing  $n_0$ .

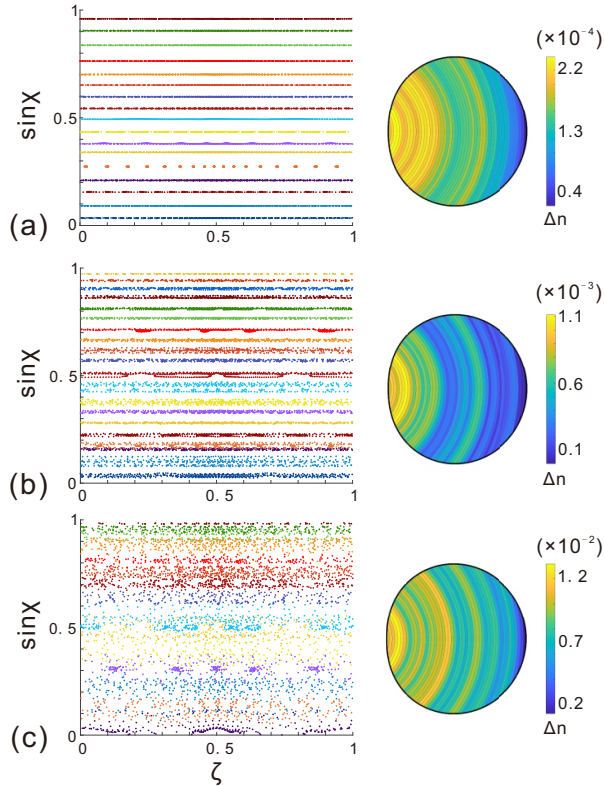


FIG. 2. Poincaré SOSs of transformed Robnik billiards with different degree of perturbation. The maximal magnitude of the perturbation is in the order of  $10^{-4}$  (a),  $10^{-3}$  (b) and  $10^{-2}$  (c). The right side shows the magnitudes of random layered perturbations.

In the following, we choose  $n_0 = 1$ , for the sake of simplicity. Interestingly, when  $\gamma = \frac{1}{4\epsilon}$ , the contour lines of  $n(x, y)$  are concentric circles with center  $(0, 0)$ , as shown in Fig. 1(b). The trajectories of the light rays can be obtained by solving the geodesic equations of the transformed space with metric  $ds^2 = g_{ij}dx^i dx^j = n^2(x, y)(dx^2 + dy^2)$ . When  $n(x, y)$  is azimuthally symmetric, an analytical solution is available, otherwise they can be solved by numerical means, such as the Runge-Kutta method (For details of calculation, see Section II of Ref.<sup>15</sup>). The lower right panels of Figs. 1(c)-(f) illustrate typical trajectories in the original or transformed billiards for two different values of  $\epsilon$ , with their corresponding  $n(x, y)$  shown in the upper right panels. One can observe a clear caustic formed by the currently curved trajectory. Because of the angle-preserved property of conformal transformations, the incident angle  $\chi$ , and consequently the tangential momentum  $\sin \chi$ , remain constant. Accordingly, the Poincaré SOS of the transformed billiard is composed of horizontal lines, indicating its integrable nature. Thus, whatever chaotic the original Robnik billiard is, one can always eliminate the occurrence of chaoticity through  $n(x, y)$  given by Eq. (3b).

In practice, there may exist systematic or random fluctuations in realizing the varying refractive index, which might hinder the transformed billiard to be perfectly integrable. It is therefore important to examine the sensitivity of this method

to small disturbances and to assess its robustness, despite the high sensitivity of chaotic systems to small perturbations. Here we are going to inspect the stability of this method against slight disturbance. Suppose that on the basis of Eq. (3b),  $n(x, y)$  is also subject to a layered-structured random perturbation  $\Delta n_i(x, y)$ <sup>23</sup>, that is, the practical distribution of refractive index in the transformed billiard is

$$n_p(x, y) = n(x, y) + \Delta n_i(x, y), \quad (x, y) \in i\text{th layer}. \quad (4)$$

Here the profiles of the layered structure conform to the contour lines of Eq. (3b), and the magnitude of layered perturbation  $\Delta n_i(x, y)$  is randomly given. As an example, in Fig. 2, we consider a transformed billiard with  $\epsilon = 0.2$  and 50 layers of perturbation, and maximal magnitude of perturbation  $[\Delta n_i(x, y)]_{\max}$  is in the order of  $10^{-4}$  (a),  $10^{-3}$  (b) and  $10^{-2}$  (c). The Poincaré SOSs of each case are demonstrated, with the magnitude of perturbation presented at the right side. It is seen that when the perturbation is small enough  $[\Delta n_i(x, y)] \lesssim 10^{-4}$ , the horizontal lines in the Poincaré section almost remain intact, revealing that the integrable property of the transformed billiard is maintained. When the perturbation increases by an order of magnitude, for an arbitrary trajectory, the previous horizontal line now expands to a strip filled with structureless grains, which indicates that every time the light ray collides on the boundary, the tangential momentum is no longer constant, but varies stochastically and chaotically within a limited range. The thicknesses of the strips vary with the initial conditions of trajectories. Despite of this phenomenon that signals the emergence of chaoticity, the structure of the phase space is basically regular. When the magnitude of perturbation further increases to the order of  $10^{-2}$ , one can observe in Fig. 2(c) that the strips are prominently broadened, and accordingly the neighboring strips overlap. In this case the degree of chaos in the transformed billiard is significant. Thus, our approach is robust to small perturbations.

So far we have demonstrated an approach of transferring a chaotic billiard into integrable, by means of a conformal transformation starting from a planar circular billiard. As a matter of fact, implementing some other landscapes of refractive index may lead to even more striking properties of the chaotic billiard. To this end, one can relate such chaotic billiards with some non-Euclidean billiards, so that special characters of the trajectories (geodesics) on the latter could be taken advantage of. Here the term "non-Euclidean billiard" refers to a surface of revolution with a specular mirror placed along its parallel (i.e., a latitude, for example, the equator). It has been proven<sup>15</sup> that a surface of revolution, described by the metric

$$ds^2 = E(\rho)d\rho^2 + G(\rho)d\theta^2 \quad (5)$$

with  $E$  and  $G$  being functions of longitudinal coordinate  $\rho$ , can be equivalently projected to a circular billiard (denoted by the polar coordinates  $r, \varphi$ ) with refractive index

$$n' [r(\rho)] = \sqrt{G(\rho)} \exp \left[ - \int^{\rho} \sqrt{\frac{E(\rho')}{G(\rho')}} d\rho' \right], \quad (6)$$

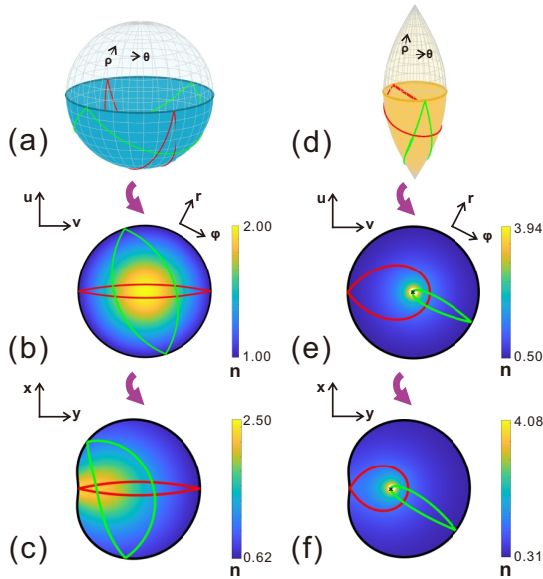


FIG. 3. (a) A sphere billiard and (d) a spindle billiard. (b,e) Distributions of refractive index in the inhomogeneous circular billiards projected from (a) and (d), respectively. (c,f) Distributions of refractive index in the inhomogeneous Robnik billiards conformally transformed from the inhomogeneous circular billiards in (b) and (e), respectively. Two typical trajectories in the sphere and spindle billiards, along with their correspondence in (b,e) and (c,f), are illustrated. Note that the refractive index approaches to infinity at positions marked by black cross, corresponding to the bottom tip of spindle which is a singularity for light, and manually left blank in (e) and (f).

through a conformal coordinate transformation

$$r = \exp \left[ \int^{\rho} \sqrt{\frac{E(\rho')}{G(\rho')}} d\rho' \right], \varphi = \theta. \quad (7)$$

Both the non-Euclidean billiard and the inhomogeneous circular billiard are integrable, owing to the rotational/azimuthal symmetry. Subsequently, the azimuthally symmetric inhomogeneous circular billiard can be further transformed to the Robnik billiard, with refractive index

$$n''(x, y) = n'(u, v) \left| \frac{dw(u, v)}{dz(x, y)} \right|. \quad (8)$$

By this means, features of geodesics on the curved surface are inherited to their counterparts in the transformed Robnik billiards. For instance, on a spherical billiard [Fig. 3(a)], with  $E(\rho) = 1$ ,  $G(\rho) = \cos^2 \rho$  and a spindle billiard [Fig. 3(d)], with  $E(\rho) = 1$ ,  $G(\rho) = R_0^2 \cos^2(\rho/R)$ , constant  $R = 2R_0$ , all the geodesics are closed, and their corresponding schemes of refractive index are shown in Figs. 3(c) and (f). On spherical billiards, any ray launching from the equator travels half an orthodrome (great circle) before its subsequent collision on the equator, and returns to the starting point in the next collision. In other words, all the trajectories on a spherical billiard retrace themselves with two collisions on the equator in each

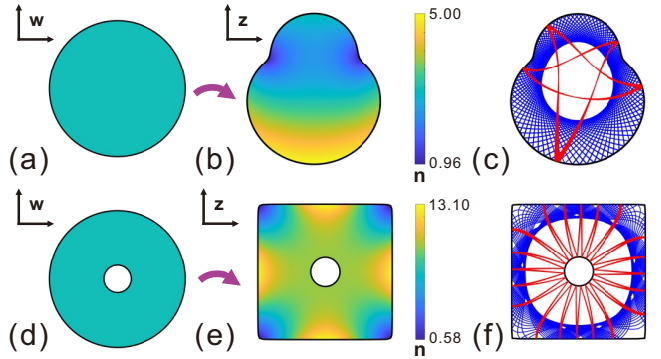


FIG. 4. Refractive index distributions in (b) a transformed calabash-shaped billiard and (e) a transformed Sinai billiard, respectively, transformed from (a) an integrable circular billiard and (d) an integrable annular billiard. Two different typical trajectories of (b) and (e) are plotted in (c) and (f), respectively. In (c), the blue trajectory is a whispering-gallery orbit, and the red one is a quasi-periodic orbit. In (f), the blue trajectory collides exclusively on the outer boundary, while the red one bounces between the inner and outer boundaries.

period. In the transformed Robnik billiard in Fig. 3(c), one can observe that any trajectory is closed and periodic, which would reveal itself in Poincaré section not as a horizontal line, but as two points. Moreover, on a spindle billiard, all the rays return to the starting point without colliding on the equator. Correspondingly, all the trajectories in the transformed Robnik billiard in Fig. 3(f) are found to be periodic and would appear in the Poincaré section as a single point.

Finally, we want to point out that our approach is not limited to the Robnik billiards. This method can be extended to arbitrary 2D chaotic billiard with various deformed boundary, providing that a proper transformation that relates it to a known integrable shape is found. This claim is further substantiated with the following two typical examples. First let us consider a calabash-shaped billiard. Its chaotic ray dynamics is confirmed by the analysis of its Poincaré SOS. Now using the idea presented above, the calabash shape can be achieved through the transformation

$$z = -\frac{i}{2} (w^3 + w^2 + 5w) \quad (9)$$

from a planar circular billiard, as shown in Fig. 4(a). Then by introducing the refractive index profile from Eq. (3a), one can finally obtain the transformed calabash-shaped billiard presented in Fig. 4(b). In Fig. 4(c), we show two typical trajectories: a whispering-gallery orbit and a quasi-periodic orbit. This manifests its integrability in such transformed calabash-shaped billiard. For billiards with other shape boundaries, one can in principle construct an analytical function, such as polynomials, of the complex variable  $w$  to fit its contour. Besides the above-mentioned focusing billiards, this method also applies for dispersing billiards with convex boundaries. As an example, when we apply the Schwartz-

Christoffel mapping<sup>24–26</sup>

$$z = \frac{1}{10} \left\{ -1 + i + \frac{2\sqrt{2}(1-i)}{\sqrt{2}K(-1) + iK\left(\frac{1}{2}\right)} \right. \\ \left. \times F \left[ i \sinh^{-1} \frac{1}{\sqrt{i\frac{1+w}{1-w} - 1}} \middle| 2 \right] \right\} \quad (10)$$

on an annular billiard, where  $F(\varphi|m)$  is the incomplete elliptic integral of the first kind with modulus  $m$ , and  $K(m)$  is the complete elliptic integral of the first kind, then we obtain the well-known Sinai billiard<sup>27</sup>. As is seen in Fig. 4(f), its inner boundary basically conserves its original shape after transformation, while the outer boundary is transformed into a square. Again, by introducing a nonuniform refractive index profile from Eq. (3a), this celebrated case of chaotic system is turned into a regular cavity, and its integrable nature is also confirmed by the analysis of its Poincaré SOS and two typical trajectories are shown in Fig. 4(f).

To summarize, we put forward an elegant method to switch off chaos in 2D flat optical billiards. By properly introducing a nonuniform distribution of refractive index, arbitrary deformed chaotic table billiards can be transformed into integrable ones. We examine the robustness of this approach against random fluctuation of refractive index. Besides the elimination of chaos, we can go one step further and turn all the trajectories to periodic orbits by providing another landscape of refractive index which is obtained via transformation from some non-Euclidean billiards. Taking advantage of special geodesics on curved surfaces, more interesting properties of transformed table billiards are to be explored. The notion of chaos switch-off and trajectory rectification could lead to a wealth of applications in photonics and laser physics. It is also interesting to consider the wave behavior in such deformed but integrable billiards obtained here via conformal coordinate transformations. The spatially varying refractive index can be realized through the optically-induced giant Kerr effect in liquid crystal<sup>28</sup>, with its landscape being provided by a spatial light modulator working in reflection. Controlling the spatial distribution of refractive index can be also implemented by the interaction of light with atoms<sup>29</sup>, ultrafast photomodulation technique<sup>30</sup> and artificial metamaterials<sup>31</sup>. We envision that these new technologies will offer interesting opportunities to manipulate light dynamics between order and chaos.

## ACKNOWLEDGMENTS

Zhejiang Provincial Natural Science Foundation of China (No. LD18A040001), the National Natural Science Foundation of China (NSFC) (No. 11974309 and 11674284), and National Key Research and Development Program of China (No. 2017YFA0304202); the CNRS support under grant PICS-ALAMO, the Israel Science Foundation (No. 1871/15,

2074/15 and 2630/20), and the United States-Israel Binational Science Foundation NSF/BSF (No. 2015694).

## DATA AVAILABILITY

The data that support the findings of this study are available from the corresponding author upon reasonable request.

## REFERENCES

1. L. M. Pecora and T. L. Carroll, *Phys. Rev. Lett.* **64**, 821 (1990).
2. E. Ott, C. Grebogi, and J. A. Yorke, *Phys. Rev. Lett.* **64**, 1196 (1990).
3. W. L. Ditto, S. N. Rauseo, and M. L. Spano, *Phys. Rev. Lett.* **65**, 3211 (1990).
4. J. U. Nöckel and A. D. Stone, *Nature* **385**, 45 (1997).
5. C. Gmachl, F. Capasso, E. E. Narimanov, J. U. Nöckel, A. D. Stone, J. Faist, D. L. Sivco, and A. Y. Cho, *Science* **280**, 1556 (1998).
6. J. Wiersig and M. Hentschel, *Phys. Rev. Lett.* **100**, 033901 (2008).
7. C. Liu, A. Di Falco, D. Molinari, Y. Khan, B. S. Ooi, T. F. Krauss, and A. Fratalocchi, *Nat. Photon.* **7**, 473 (2013).
8. C. Liu, A. Di Falco, and A. Fratalocchi, *Phys. Rev. X* **4**, 021048 (2014).
9. C. Liu, R. E. C. van der Wel, N. Rotenberg, L. Kuipers, T. F. Krauss, A. Di Falco, and A. Fratalocchi, *Nat. Phys.* **11**, 358 (2015).
10. Y. Kim, S. -Y. Lee, J. -W. Ryu, I. Kim, J. -H. Han, H. -S. Tae, M. Choi, and B. Min, *Nat. Photonics* **10**, 647 (2016).
11. X. Jiang, L. Shao, S. -X. Zhang, X. Yi, J. Wiersig, L. Wang, Q. Gong, M. Lončar, L. Yang, Y. -F. Xiao, *Science* **358**, 344 (2017).
12. S. Bittner, S. Guazzotti, Y. Zeng, X. Hu, H. Yilmaz, K. Kim, S. S. Oh, Q. J. Wang, O. Hess, and H. Cao, *Science* **361**, 1225 (2018).
13. L. A. Bunimovich, *Nonlinearity* **31**, R78 (2018).
14. D. Wang, C. Liu, S. Zhang, and C. T. Chan, *Nanophotonics* **9**, 3367 (2020).
15. C. Xu, I. Dana, L. -G. Wang, P. Sebbah, arXiv: 2010.12220 (2020).
16. L. Xu and H. Chen, *Nat. Photon.* **9**, 15 (2015).
17. L. Fan, X. Yan, H. Wang, and L. V. Wang, *Sci. Adv.* **7**, eabc8448 (2021).
18. R. Bruck, C. Liu, O. L. Muskens, A. Fratalocchi, and A. Di Falco, *Laser Photonics Rev.* **10**, 688 (2016).
19. M. Robnik, *J. Phys. A: Math. Gen.* **16**, 3971 (1983).
20. The radius of the forbidden area is determined by the value of  $\sin \chi$  for a unit circular billiard. Since all the reflected light rays have the same reflected angles equal to the incident ones, the minimal distance from the center to any light ray is equal to the vertical distance which is  $\sin \chi$ .
21. M. C. Gutzwiller, *Chaos in Classical and Quantum Mechanics* (New York, Springer-Verlag, 1990).
22. Y. Kim, S. -Y. Lee, J. -W. Ryu, I. Kim, J. -H. Han, H. -S. Tae, M. Choi, and B. Min, *Nat. Photon.* **10**, 647 (2016).
23. Note that the distribution of refractive index in Eq. (3b) is concentric with the origin (0,0) although the deformed shape is not centered on that origin. From the fabrication point of view, the same value of refraction index is controlled by the same control parameter, thus the random perturbation of refractive index is usually of a layered-structured form.
24. M. Schmiele, V. S. Varma, C. Rockstuhl, and F. Lederer, *Phys. Rev. A* **81**(3), 033837 (2010).
25. C. Ren, Z. Xiang, and Z. Cen, *Appl. Phys. Lett.* **97**(4), 044101 (2010).
26. L. Tang, J. Yin, G. Yuan, J. Du, H. Gao, X. Dong, Y. Lu, and C. Du, *Opt. Express* **19**, 15119 (2011).
27. Ya. G. Sinai, *Russ. Math. Surv.* **25**, 137 (1970).
28. I. C. Khoo, *J. Opt. Soc. Am. B* **25**, A45 (2011).
29. M. O. Scully and M. S. Zubairy, *Quantum Optics* (Cambridge University Press, 1997).
30. R. Bruck, B. Mills, B. Troia, D. J. Thomson, F. Y. Gardes, Y. Hu, G. Z. Mashanovich, V. M. N. Passaro, G. T. Reed, and O. L. Muskens, *Nat. Photon.* **9**, 54 (2015).
31. Y. Liu and X. Zhang, *Chem. Soc. Rev.* **40**, 2494 (2011).